

Uplink Capacity and Interference Avoidance for Two-Tier Cellular Networks

Vikram Chandrasekhar and Jeffrey G. Andrews
Wireless Networking and Communications Group
Department of Electrical and Computer Engineering
The University of Texas at Austin

Email: cvikram@mail.utexas.edu, jandrews@ece.utexas.edu

Abstract— This paper presents an uplink capacity analysis and interference avoidance technique for a femtocell based two-tier DS-CDMA network using shared spectrum. Assuming randomly distributed macrocell users and femtocell base stations (BS), we evaluate a network-wide area spectral efficiency metric called the operating contour (OC) defined as the feasible combinations of the average macrocell users and femtocell BS per cell-site that meet a target outage constraint ϵ . A contribution of this work is an accurate characterization of the uplink outage probability taking cross-tier power control, path-loss and shadowing effects into account. We show that a time-hopped CDMA physical layer coupled with sectorized receive antennas shows dramatic performance improvements in both light and heavily loaded two-tier networks, relative to a split spectrum two-tier network with omnidirectional femtocell antennas. These results provide insights into design of robust shared spectrum two-tier networks which achieve high area spectral efficiency.

I. INTRODUCTION

Two-tier femtocell networks (Figure 1) are in the process of being deployed to improve cellular capacity. A femtocell serves as a small range data access point with limited user capacity for stationary or low-mobility users. We model each femtocell as consisting of a fixed number of users. The femtocell radio range (10 – 50 metres) is much smaller than the macrocell radius (300 – 2000 metres). Users transmitting to femtocells experience superior signal reception and lower their transmit power, consequently prolonging battery life. The implication is that femtocell users cause less co-channel interference (CCI) to neighboring femtocells and other macrocell users. Additionally, a two-tier network offsets the burden on the macrocell BS, provided femtocells are judiciously placed in traffic hot-spots, improving network capacity and QoS.

A. Related work

Prior research on two-tier networks has largely focused on analyzing the network capacity when a single microcell is embedded inside a macrocell. In the context of our work, these microcell sizes are comparable to those of the macrocell (typically of the order of a few hundred metres). Kishore et al. [1] derived analytic methods to analyze different methods of tier-selection and the OC for a two-tier network with a single embedded microcell. However, this paper does not show how the network capacity is affected due to the relative location of the microcell inside the macrocell.

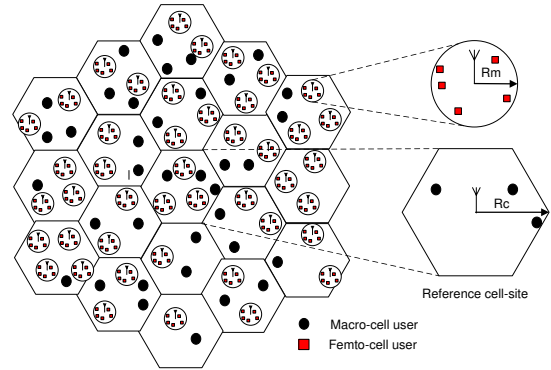


Fig. 1. A femtocell based two-tier CDMA network

Zemlianov et al. [2] perform a capacity-type analysis for deriving per-user throughput regimes in ad-hoc networks with infrastructure support. In contrast, our work assumes fixed bit-rate per user and focusses on maximizing the OC that a two-tier network can sustain for a target outage constraint. Wu et al. [3] consider a network comprising a large hexagonal macrocell and smaller hexagonal microcells. This paper indicates that the near-far effect degrades system performance for both microcells and the larger macrocell. Consequently, they conclude that it may be more practical to split the RF spectrum between each tier to maximize the network OC. Through our paper, we show a higher user capacity by enforcing *higher spatial reuse* through small sized femtocells and *interference avoidance* by way of antenna sectoring and TH-CDMA in each tier.

B. Contribution

We consider a two-tier network with universal frequency reuse and small range femtocells. From a network-wide area spectral efficiency perspective, it is more beneficial to have small sized femtocells owing to increased spatial reuse and reduced transmit power.

The user capacity of the two-tier network is evaluated using a network-wide area spectral efficiency metric called the network operating contours (OC); defined as the combinations of average number of macrocell users and femto cell BSs

per cellsite that satisfy a target outage constraint ϵ . The key takeaway from this paper is that interference avoidance techniques such as antenna sectoring and TH-CDMA physical layer transmission can help single frequency two-tier networks achieve higher user capacity, thereby avoiding the design of protocols which require the mobile to sense the spectrum (in split spectrum networks).

A novel contribution in this paper relates to analyzing outage probabilities for a two-tier network taking the *cellular geometry* and *near-far effects* into account. For doing so, assume that the macrocell users and femtocell BS are randomly distributed on the plane as a Homogeneous Spatial Poisson Point Process (SPPP). We utilize the properties of Poisson shot-noise processes (SNP) described in [4] and void probabilities of Poisson processes [5] for deriving uplink outage probabilities. Through simulations, the outage analysis is shown to be accurate through simulations, indicating the applicability of our model in this context.

For a split spectrum two-tier network, the cross-tier CCI seen at any femtocell is location independent as the femtocell users and macrocell users are orthogonal. However, for a shared spectrum two-tier network, closed loop macrocellular power control causes higher CCI at a corner femtocell relative to an interior femtocell. Even taking worst-case cross-tier interference at femtocell into account, simulation results reveal that interference avoidance results in an 4x increase in femtocell BS density over split spectrum two-tier networks.

We would like to mention that the Poisson model of user distribution has been confirmed in empirical studies and used in prior work. For example, Chan and Hanly [6] have used the Poisson model for describing the out-of-cell interference in a CDMA cellular network. The Poisson process is a natural model arising from highly mobile macrocellular users and placement of femtocell BS in densely populated downtown areas.

II. SYSTEM MODEL

Assume that the macrocell users are distributed on \mathcal{R}^2 according to a homogeneous SPPP Φ_c of intensity λ_c . The femtocell BS's are overlaid on top of the existing macrocell network and form a homogeneous SPPP Φ_f with intensity λ_f . After tier-selection, each femtocell comprises $N > 1$ users in a circular coverage area of radius R_f , $R_f \ll R_c$. To maximize user capacity per cell, it is desirable to have $\lambda_f > \lambda_c$. Defining $A \equiv 2.6R_c^2$ to be the area of a regular hexagon of side R_c , the average number of macrocell users and femtocell BS's per hexagonal cell-site are given as $N_c = \lambda_c A$ and $N_f = \lambda_f A$ respectively.

A. Physical layer transmission and antenna sectoring

Assume that the users in each tier employ DS-CDMA uplink transmission with processing gain G to communicate with the BS. Suppose that the CDMA period $T = GT_c$ is divided into N_{hop} hopping slots of duration $T_h = T/N_{hop}$ each. If each macrocell user and each femtocell (all N users in femtocell hop together) independently chooses to transmit

over any one slot, then users in each tier mitigate intra- and cross-tier interference by ‘‘thinning’’ the respective Poisson processes by a factor of N_{hop} [5]. If $N_{hop} > 1$, users in each tier effectively sacrifice a portion of their processing gain for combating interference by thinning the intensity of the Poisson field. Assume sectorized antenna reception in both the macrocell and femtocell BS, with N_{sec} sectors per antenna.

B. Uplink Power Control

The users in each tier deploy closed-loop uplink power control to adjust for propagation loss and log-normal shadowing. The macrocell and femtocell receive powers are denoted as P_r^c and P_r^f respectively. Short-term fading effects are ignored for analytical convenience, with the assumption that they are dealt using robust reception techniques.

C. Channel Model and Interference

The channel is represented as a combination of path-loss and log-normal shadowing. The path-loss exponents are denoted by α (outdoor macrocell transmission and cross-tier interference) and β (indoor femtocell transmission) while the log-normal shadowing is parametrized by its standard deviation σ_{dB} .

Through uplink power control, a macrocell user transmitting at a distance x from the reference macrocell BS C chooses a transmit power level $P_t^c = P_r^c/g_c(x)$. Here $g_c(x)$ is the attenuation function defined as $g_c(x) = K_c(d_{0c}/x)^\alpha \theta_C$ where $10 \log_{10} \theta_C \sim LN(0, \sigma_{dB})$ is the log-normal shadowing from user to C, $K_c \triangleq [c/(4\pi f_c d_{0c})]^2$ is a unit-less constant that depends on wavelength of RF carrier c/f_c and outdoor reference distance d_{0c} . Similarly, a femtocell user at a distance x from femtocell BS F chooses transmit power $P_t^f = P_r^f/g_f(d)$, where $g_f(d) = K_f(d_{0f}/x)^\beta \theta_F$ and $K_f \triangleq [c/(4\pi f_c d_{0f})]^2$. Here d_{0f} is the reference distance for calculating indoor propagation loss. Note that in reality, K_c, K_f are empirically determined.

The interference in each tier can be grouped into five categories:

- *Macrocell interference at macrocell BS:* Through power control, all in-cell macrocell users are received with constant power P_r^c , hence the intra-tier interference $I_{c,in}$ is Poisson distributed. Interference from macrocell users outside the reference macrocell $I_{c,out}$ is assumed to be Gaussian distributed [6].
- *Femtocell interference at macrocell BS:* The cumulative interference caused by femtocells at the reference macrocell BS C is represented by the Poisson SNP $I_{c,f} = \sum_{F_i \in \Phi_f} Q_f \psi_i |x_i|^{-\alpha}$, where femtocell F_i with N users is located at position x_i relative to C. Here $Q_f = \frac{P_r^f |R_f|^\beta}{K_f d_{0f}^\beta} K_c d_{0c}^\alpha$ and $\psi_i = \sum_{l=1}^N \theta_{l,C}/\theta_{l,F_i}$ represents the effective shadowing gain. We make two important assumptions:

AS 1: For small-sized femtocells, the center of any microcell or macrocell BS sees interference from any other microcell as a *point-source* of interference. This

assumption is valid for small R_f and helps simplify outage event analysis in each tier.

AS 2: When analyzing the interference caused by a femtocell at any other location outside femtocell, model the N users per femtocell to transmit with maximum power. This is for analytical tractability and modeling worst-case interference.

- **Neighboring femtocell interference at femtocell BS:** As the femtocell locations form a homogeneous SPPP, the interference caused at a femtocell F_j from other femtocells is a Poisson SNP. So, $I_{f,f} = \sum_{F_i \in \hat{\Phi}_f, F_i \neq F_j} Q_f \psi_i |x_i|^{-\alpha}$, where $|x_i|$ refers to the distance between (F_i, F_j) and $\psi_i = \sum_{l=1}^N \theta_{l, F_j} / \theta_{l, F_i}$.
- **Interference from other femtocell users at femtocell BS:** The worst-case scenario is considered, wherein all N users inside femtocells are transmitting. Consequently, the interference at the femtocell BS caused by other femtocell users equals $(N-1)P_r^f$.
- **Macrocell interference at femtocell BS:** We assume that the femtocell BS is located on the hexagonal axis, and consider only the effect of in-cell macrocellular CCI. Interference caused by macrocellular users at femto cell is not stationary, clearly it is a function of the femto-cell position. The overall macrocell CCI at femto cell is lower-bounded as $I_{f,c} = \sum_{i \in \Phi_c \text{ over } \mathbf{H}} P_r^c \psi_i (|y_i|/|x_i|)^{-\alpha}$ where \mathbf{H} denotes the hexagonal cell-site region and $10 \log_{10} \psi_i \sim N(0, \sqrt{2}\sigma_{dB})$, (x_i, y_i) represent the distances of macrocell user i to the macrocell BS and femtocell BS respectively.

III. TIER OUTAGE PROBABILITY

To derive the operating contours, we formulate an uplink outage probability constraint per tier. Define (N_f, N_c) as the average number of femtocell BS's and macrocell users per cell-site. A user experiences outage if the received Signal-to-Interference Ratio (SIR) is below a threshold γ . Any feasible combination $(\tilde{N}_f, \tilde{N}_c)$ satisfies the outage probability requirement $P_{out}^f \leq \epsilon$, $P_{out}^c \leq \epsilon$ in each tier.

The outage probabilities $P_{out}^c(N_f, N_c)$ [$P_{out}^f(N_f, N_c)$] are defined as the probabilities that the cumulative interference experienced by a macrocellular user [femtocell user] at the BS exceeds γ . Note that the interference terms arise from thinned Poisson processes with intensities $\hat{\lambda}_c = \lambda_c / (N_{hop} \cdot N_{sec})$ and $\hat{\lambda}_f = \lambda_f / (N_{hop} \cdot N_{sec})$ respectively. Assuming the PN code cross-correlation equals $1/G$, define

$$P_{out}^c(N_f, N_c) = \Pr\left(\frac{G/N_{hop}P_r^c}{I_{c,in} + I_{c,out} + I_{c,f}} \leq \gamma \mid |\hat{\Phi}_c| \geq 1\right)$$

$$P_{out}^f(N_f, N_c) = \Pr\left(\frac{G/N_{hop}P_r^f}{(N-1)P_r^f + I_{f,f} + I_{f,c}} \leq \gamma \mid |\hat{\Phi}_f| \geq 1\right) \quad (1)$$

where $|\cdot|$ denotes size of a set and $(\hat{\Phi}_c, \hat{\Phi}_f)$ denotes the thinned SPPPs. The OCs for the macrocell [femtocell] are obtained by

computing the maximum average femtocell BS's [macrocell users] meeting the outage constraint ϵ . More formally

$$\tilde{N}_f(N_c) = \sup\{N_f : P_{out}^c(N_f, N_c) \leq \epsilon\}$$

$$\tilde{N}_c(N_f) = \sup\{N_c : P_{out}^f(N_f, N_c) \leq \epsilon\} \quad (2)$$

The OCs for the two-tier network are obtained corresponding to those combinations of (N_c, N_f) that satisfy both constraints in (1). We shall use the following theorems for outage probability analysis in each tier.

Theorem 1: For small femtocell sizes, the femtocell interference terms $I_{f,f}, I_{c,f}$ are distributed as a Poisson SNP $Y = \sum_{i \in \hat{\Phi}_f} Q_f \psi_i |x_i|^{-\alpha}$ with iid $\psi_i \sim F_\psi$. In particular, if the outdoor path-loss exponent $\alpha = 4$, then Y follows a Levy-stable distribution with stability exponent $1/2$, whose pdf and CDF are given as,

$$f_Y(y) = \sqrt{\frac{\kappa_f}{\pi}} y^{-3/2} e^{-\kappa_f/y}, F_Y(y) = \text{erfc}\left(\sqrt{\frac{\kappa_f}{y}}\right) \quad (3)$$

where $\kappa_f = \frac{\hat{\lambda}_f^2 \pi^3 Q_f (\mathbf{E}[\psi^{1/2}])^2}{4}$

Proof: See [4]. ■

The theorems given below are stated without proof. Using Theorem 1, the macrocellular outage probability is formulated using the following theorem:

Theorem 2: Let outdoor path-loss exponent $\alpha = 4$. With Poisson in-cell macrocell interference $I_{c,in}$, Gaussian out-of-cell interference $I_{c,out}$ and Levy-stable femtocell interference $I_{c,f}$, the outage constraint at macrocell is given by,

$$\epsilon \geq P_{out}^c = 1 - \frac{1}{1 - e^{-\hat{\lambda}_c A}} \sum_{m=1}^{\lfloor \rho_c P_r^c \rfloor} \frac{e^{-\hat{\lambda}_c A} \hat{\lambda}_c A^m}{m!} G(\tilde{\rho}_c) \quad (4)$$

where $\rho_c = P_r^c G / (N_{hop} \gamma)$, $\tilde{\rho}_c = \rho_c - (m-1)P_r^c$ and $G(\omega) = \int_0^\omega f_{I_{c,out}}(\tilde{\rho}_c - y) F_{I_{c,f}}(y) dy$

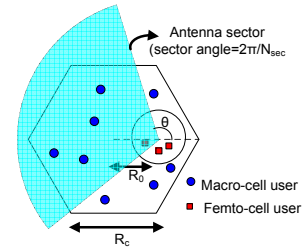


Fig. 2. Femtocell antenna alignment w.r.t hexagonal axis

For computing outage probability at any femtocell located at distance R_0 from macrocell BS, assume that the femtocell receive antenna is aligned at angle θ w.r.t the hexagonal axis (Figure 2). The following theorem obtains a lower bound on the outage probability at an femtocell considering the void probabilities of the set of dominant macrocellular interferers.

Theorem 3: Denote $\psi = \sum_{j=1}^n \psi_j$ where $10 \log_{10} \psi_j \sim LN(0, \sqrt{2}\sigma_{dB})$. At any femtocell located at distance $0 \leq$

$R_0 \leq R_c$ from macrocell BS along hexagonal axis, the CCDF of the macrocellular interference $I_{f,c}$ over one sector is lower bounded as $\bar{F}_{I_{f,c}}(y) \geq \bar{F}_{I_{f,c}}^{lb}(y)$, with

$$F_{I_{f,c}}^{lb}(y) = \exp \left\{ -\frac{\lambda_c}{N_{hop}} \int \int_{\mathbf{H}^{int}} \bar{F}_\psi \left(\frac{yr^{-\alpha}}{|re^{i\phi} + R_0|^{-\alpha}} \right) r dr d\phi \right\} \quad (5)$$

where F_ψ, \bar{F}_ψ are the CDF, CCDF of ψ and \mathbf{H}^{int} denotes the portion of the hexagonal cell-site enclosed between $\theta \leq \phi \leq \theta + 2\pi/N_{sec}$. In particular, for a corner femtocell $R_0 = R_c$ and omnidirectional femtocell antenna $N_{sec} = 1$, the CCDF of $I_{f,c}$ is lower bounded as $\bar{F}_{I_{f,c}}^{cor}(y) \geq \bar{F}_{I_{f,c}}^{cor,lb}(y)$, where

$$F_{I_{f,c}}^{cor,lb}(y) = \exp \left\{ -3 \frac{\lambda_c}{N_{hop}} \int \int_{\mathbf{H}} \bar{F}_\psi \left(\frac{yr^{-\alpha}}{|re^{i\phi} + R_0|^{-\alpha}} \right) r dr d\phi \right\} \quad (6)$$

where \mathbf{H} refers to the region comprising the reference hexagonal site.

Using Theorems 1 and 3, the femtocell outage constraints can be formulated as given in the following theorem.

Theorem 4: Let outdoor path-loss exponent $\alpha = 4$. For low outage regimes, the femtocell outage probability is lower bounded as,

$$\epsilon \geq P_{out}^f \geq \bar{F}_{I_{f,f}}(\rho_f) + \int_0^{\rho_f} \ln(F_{I_{f,c}}^{lb}(y)) f_{I_{f,f}}(\rho_f - y) dy \quad (7)$$

where $\rho_f = P_r^f [G/(N_{hop}\gamma) - (N - 1)]$.

IV. RESULTS

System parameters are shown in Table I. The overall set-up consists of a reference hexagonal cell-site surrounded by 18 macrocells to consider the effects of two rings of interferers and $2\pi/3$ sectored receive antennas at each macrocell BS. The mean and variance of the Gaussian out-of-cell interference $I_{c,out}$ were empirically estimated. In Figs 3, 4, the solid black curves show the simulation results, and the dotted colored curves show the results of analysis.

TABLE I
SYSTEM PARAMETERS

Description	Value
Processing Gain G	128
Target SIR γ	2 [C/I=3 dB]
Target Outage Probability ϵ	0.1
Macro/Femtocell Radius R_c, R_f	500, 20 meters
Users per femtocell N	5
Hopping slots N_{hop}	1, 2, 4
Path-loss exponents, α, β	4, 2
Log-normal shadowing, σ_{dB}	4
Macrocell receive power P_r^c	1
Femtocell receive power P_r^f	1, 10, 100
Reference distances d_{0c}, d_{0f}	100, 5 meters
Carrier frequency f_c	2 GHz

Figure 3 shows the effects of sectored femtocell antenna reception ($N_{sec} > 1$) and varying antenna alignment angle θ

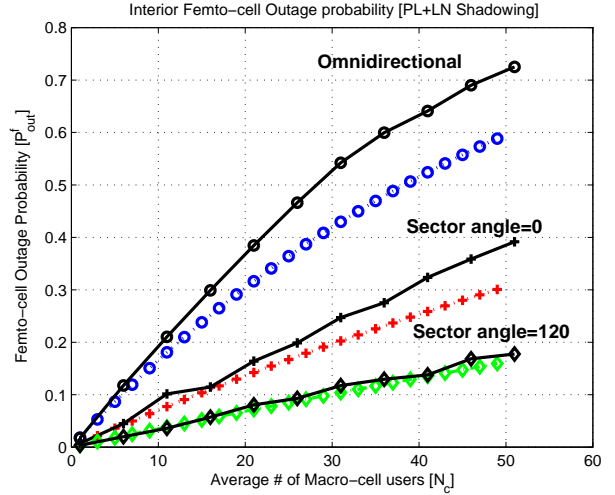


Fig. 3. Effect of antenna sectoring N_{sec} and alignment (θ) in femtocell

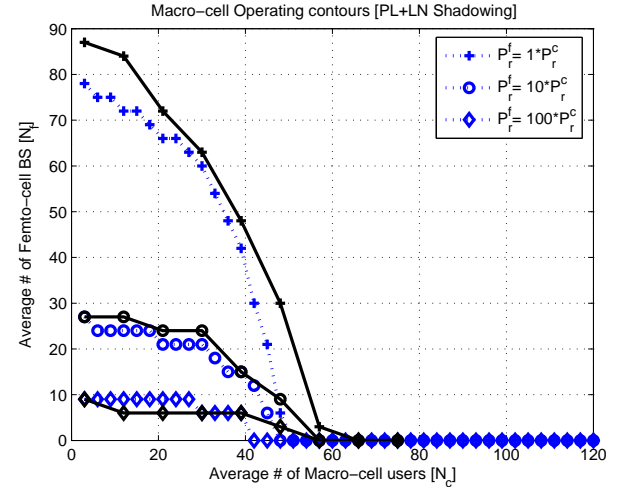


Fig. 4. Macrocell operating contours, $N_{hop} = 1, N_{sec} = 3$

on femtocell performance (adjacent femtocell interference $I_{f,f}$ is not considered). Three antenna configurations are evaluated corresponding to outage performance of an omnidirectional femtocell ($N_{sec} = 1$) and outage performance in each antenna sector ($N_{sec} = 3$) when the sectors are aligned at $\theta = 0, 2\pi/3$ radians with the hexagonal axis. The dotted lines are obtained by evaluating the outage lower bound $F_{I_{f,c}}^{lb}(\cdot)$ using (5), while the solid lines were obtained by computing actual outage probabilities through simulation. First, there is a noticeable benefit of sectoring antennas in femtocell. Next, the tightness of the theoretical lower bound (5) in the low outage regime shows that the cross-tier macrocell CCI $I_{f,c}$ is dominated by the nearest macrocell interferers. This result agrees with the conclusions in [7].

Figure 4 plots the macrocell OC in the case when no hopping takes place ($N_{hop} = 1$). The blue dotted lines

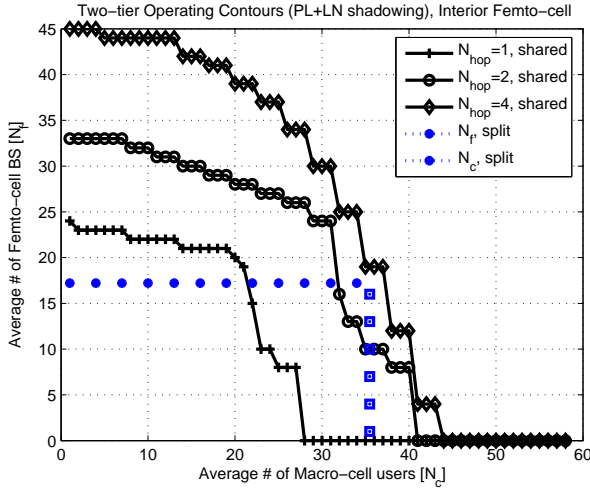


Fig. 5. Network operating contours for different hopping slots, interior femtocell, $\frac{P_r^f}{P_r^c} = 10$, $N_{sec} = 3$, $N = 5$ users/femto-cell

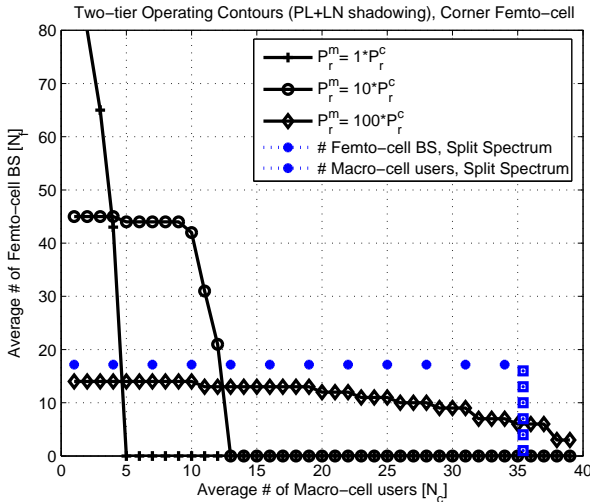


Fig. 6. Network operating contours, corner femtocell $N_{hop} = 4$, $N_{sec} = 3$, $N = 5$ users/femto-cell

correspond to the theoretical results obtained using Theorems 2 and 4. It is evident (Figure 4) that smaller $\frac{P_r^f}{P_r^c}$ results in higher N_f due to smaller femtocell CCI from the macrocell perspective.

Finally, Figs 5 and 6 plot the two-tier OCs when users in each tier employ TH-CDMA. The black solid lines correspond to the OCs of a shared spectrum two-tier network shared spectrum which uses TH-CDMA and sectored femtocell antennas ($N_{sec} = 3$). The blue dotted lines correspond to a split spectrum two-tier network with omnidirectional femtocell and no hopping. Assuming $\frac{P_r^f}{P_r^c} = 10$ and varying N_{hop} for the shared spectrum network, Figure 5 shows that an interior femtocell can achieve higher user density when compared to the split spectrum network. From Figure 6, with $\frac{P_r^f}{P_r^c} = 1$,

even the worst-case femtocell location (highest macrocell CCI) guarantees a 4x higher femtocell density for lightly loaded macrocellular regions.

V. CONCLUSION

This paper has presented an uplink capacity analysis and an interference avoidance technique for a femtocell based shared spectrum two-tier DS-CDMA network. We derive exact outage expressions for macrocell outage probability and tight lower bounds on the CCDF of the interference seen at a femtocell. We show that a time-hopped CDMA physical layer coupled with sectorized receive antennas consistently outperforms a split spectrum two-tier network with omnidirectional femtocell antennas. Considering the worst-case interference at a corner femtocell, a 4x improvement in femtocell density is observed for light-to-moderately loaded macrocell networks. Future work should consider varying the femtocell size with distance from the macrocell center and evaluating impact of tier-selection to mitigate cross-tier CCI.

ACKNOWLEDGEMENT

We acknowledge Dr. Alan Gatherer and Dr. Zukang Shen from Texas Instruments for their valuable input and sponsorship of this research.

REFERENCES

- [1] S. Kishore, L. Greenstein, H. Poor, and S. Schwartz, "Uplink user capacity in a CDMA macrocell with a hotspot microcell: exact and approximate analyses," *IEEE Transactions on Wireless Communications*, vol. 2, no. 2, pp. 364–374, Mar. 2003.
- [2] A. Zemplianov and G. de Veciana, "Capacity of ad hoc wireless networks with infrastructure support," *IEEE Journal on Selected Areas in Communications*, vol. 23, no. 3, pp. 657–667, Mar. 2005.
- [3] J.-S. Wu, J.-K. Chung, and M.-T. Sze, "Analysis of uplink and downlink capacities for two-tier cellular system," *IEE Proceedings- Communications*, vol. 144, no. 6, pp. 405–411, Dec. 1997.
- [4] S. Lowen and M. Teich, "Power-law shot noise," *IEEE Transactions on Information Theory*, vol. 36, no. 6, pp. 1302–1318, Nov. 1990.
- [5] J. Kingman, *Poisson Processes*. Oxford University Press, 1993.
- [6] C. C. Chan and S. Hanly, "Calculating the outage probability in a CDMA network with spatial poisson traffic," *IEEE Transactions on Vehicular Technology*, vol. 50, no. 1, pp. 183–204, Jan. 2001.
- [7] S. Weber, X. Yang, J. Andrews, and G. de Veciana, "Transmission capacity of wireless ad hoc networks with outage constraints," *IEEE Transactions on Information Theory*, vol. 51, no. 12, pp. 4091–4102, Dec. 2005.